Neutron Star Interior Composition ExploreR
NICER

Bev LaMarr (MIT) for the NICER team.

NICER Payload (http://heasarc.gsfc.nasa.gov/docs/nicer/slides/NICER_Science_Overview.pdf)

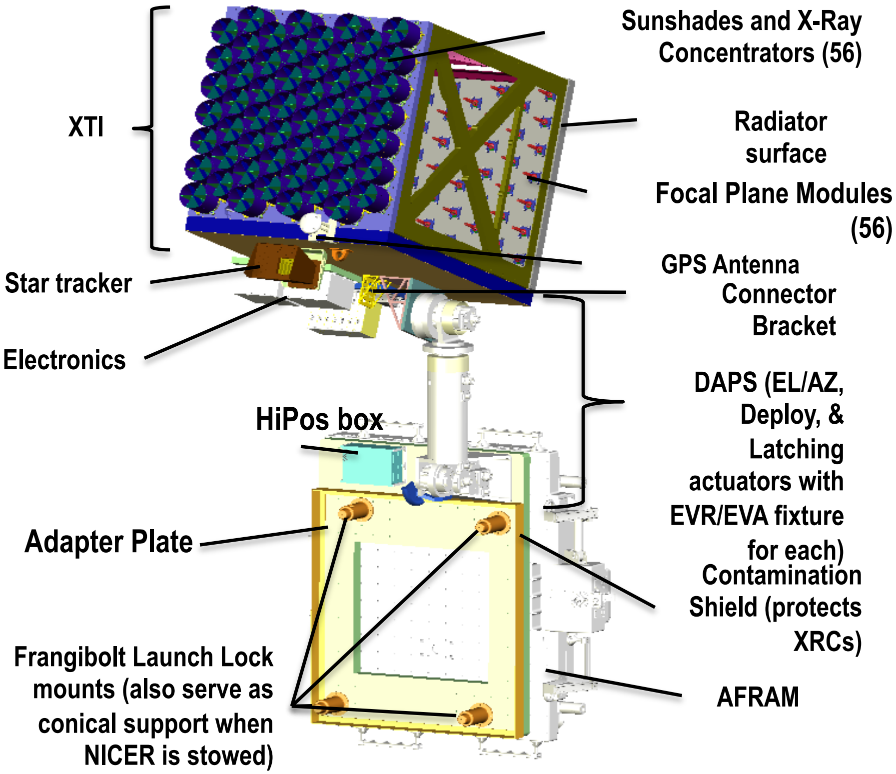

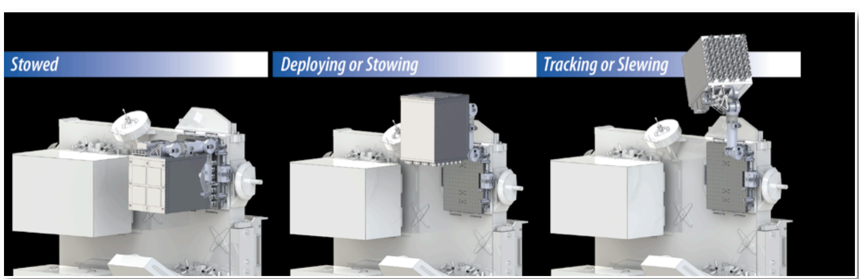

- X-ray Timing Instrument (XTI)
  - *Assembly of 56 X-ray concentrators and detectors*
  - *Detects individual X-ray photons, returns energy and time of arrival*
  - *Held together in the Instrument Optical Bench*
- Straightforward thermal system
  - *Maintains thermal-mechanical alignment*
- Pointing System
  - *Composed of high-heritage components*
  - *Allows the XTI to track pulsars*
  - *Slews XTI between targets*
- C&DH
  - *Digital interface to ISS for commands, data*
  - *Supports pointing system*
- *Flight Releasable Attachment Mechanism*
  - *Electrical & mechanical interface to ISS and transfer vehicle*
  - *Provided by ISS program*

NICER will deliver an unprecedented combination of sensitivity, time resolution, and energy resolution

- **Spectral band: 0.2–12 keV**
  - ***Well matched to neutron stars***
  - ***Overlaps RXTE and XMM-Newton***
- **Timing resolution: 100 nsec RMS absolute**
- **Energy resolution: 2% @ 6 keV**
- **Angular resolution: 6 arcmin (non-imaging FOV)**
- **Sensitivity, 5σ: 5.3 x 10^{-14} erg/s/cm^2**
  - ***0.5–10 keV in 10 ksec (Crab-like spectrum)***

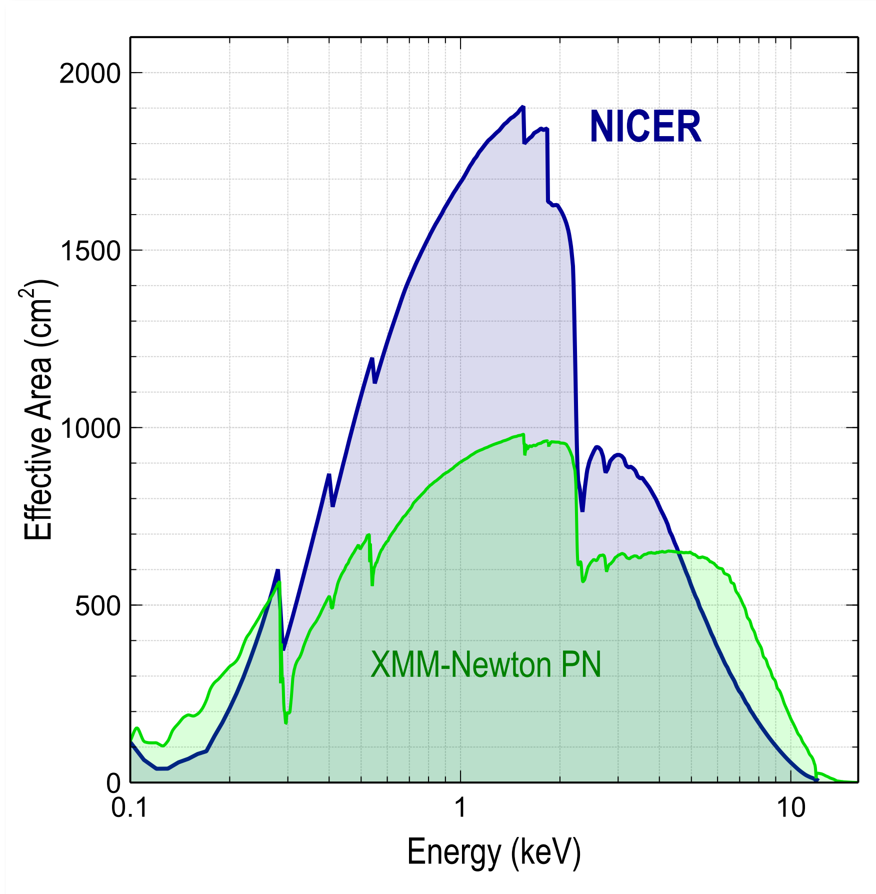

X-ray Concentrators (56)

Focal Plane Modules (56)

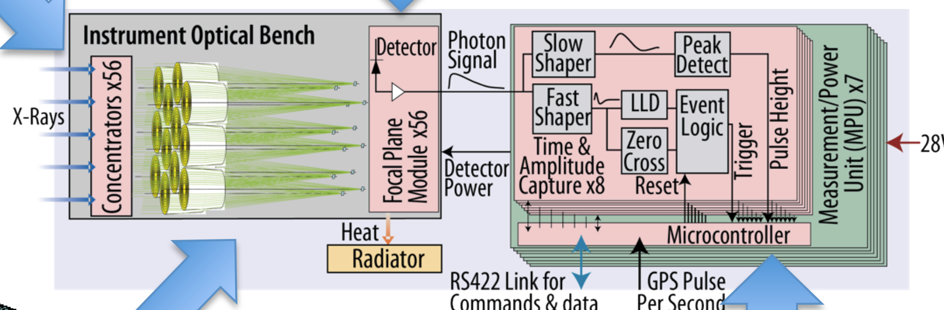

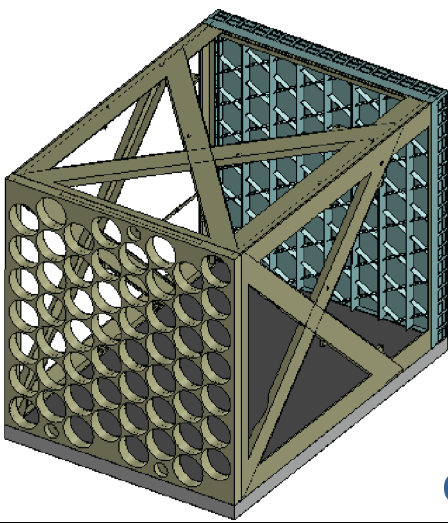

Instrument Optical Bench

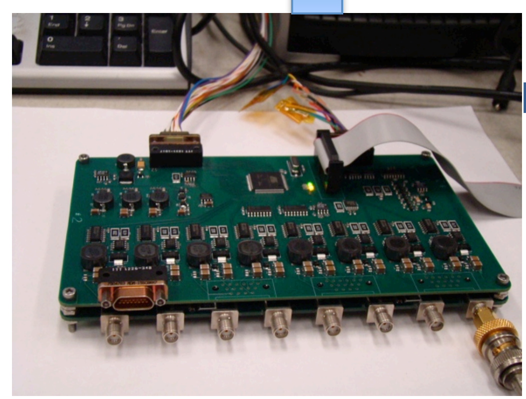

Measurement Power Units (7)

Silicon Drift Detector structure

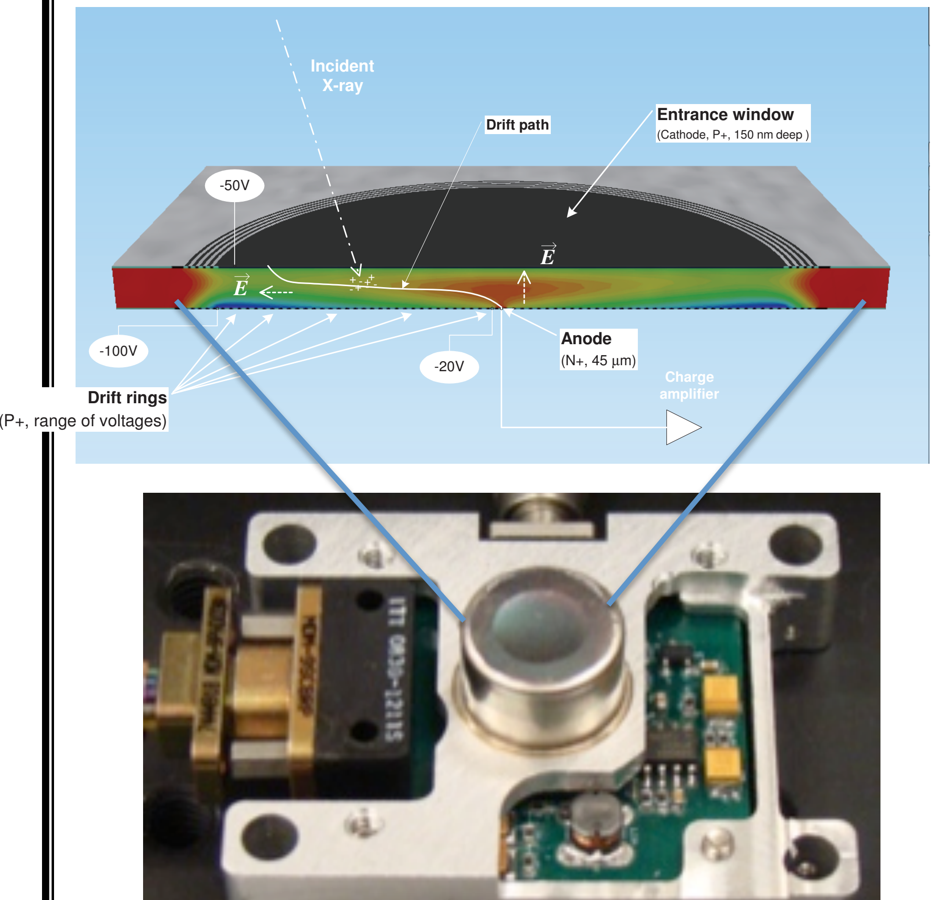

Thin p+ region at the top is biased to approximately -50 V.

This p-n junction fully depletes 500 micron thick n-type silicon bulk.

N+ anode in the center at the bottom stays at near zero potential (virtual zero).

Concentric p+ rings at the bottom provide lateral field that pulls electrons towards anode.

Anode is connected to the input of charge sensitive amplifier.

Drift time of electron cloud depends on the distance to anode.

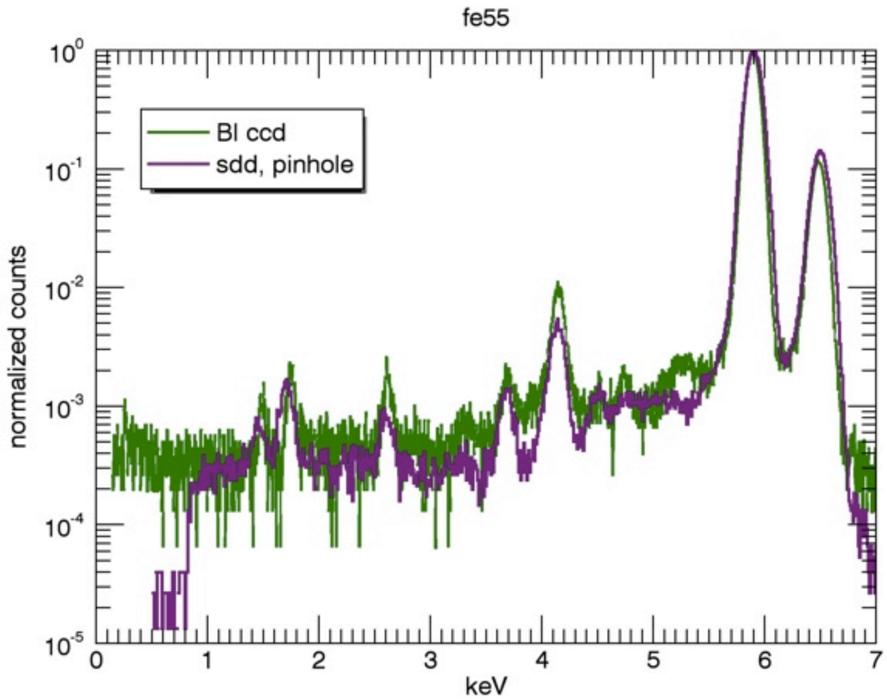

The spectrum derived from the slow channel amplitudes is comparable to a CCD.

Calibration Challenges

- 56 flight detectors (plus 8 spares)
- 7 MPUs (plus 2 spares; with late delivery, so that most of calibration is done with an Engineering MPU)
- Extraordinarily Fast Detectors (timing done with 40 ns clock ticks)

Specialized Calibration Tasks

- Fully characterize throughput, energy resolution, and redistribution over 0.2 to 12 keV.
- Measure offsets between signal hold times and true event times for both pulse analysis chains
- Measure delays for events that are outside the collimator, to help reject background events.

Planned Ground Tests

All FPMs

TEC Test
Trigger Noise
Low Energy Spectrum
Background & Dark Optical
Window Test
Long Background Test
MXS Spectrum
Fast Chain Timing
Slow Chain Timing
Flux Linearity
Clean MXS Line Spectrum

Select FPMS

Performance at -45C
Performance at -50C
Performance at -60 C
Response to MeV Gamma Rays
Timing with Pinhole Cap
Extensive Pinhole Scans
Absolute Throughput
Broadband Window
Transmission

- **Custom Calibration Chamber**
  - Allows 8 detectors at a time
  - Modulated X-ray Source (MXS) from GSFC: pulsed lines from .28 keV to 8.9 keV
  - Testing of flight detectors will begin this month

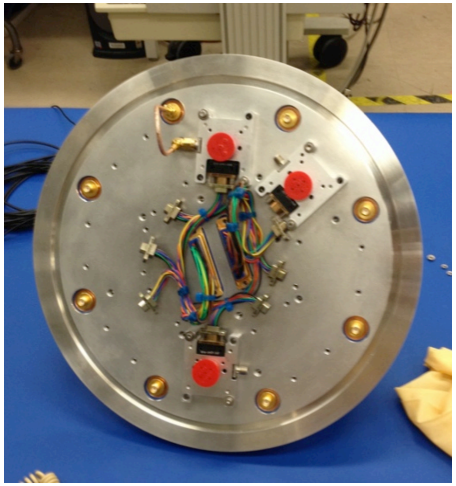

Partially populated backplate

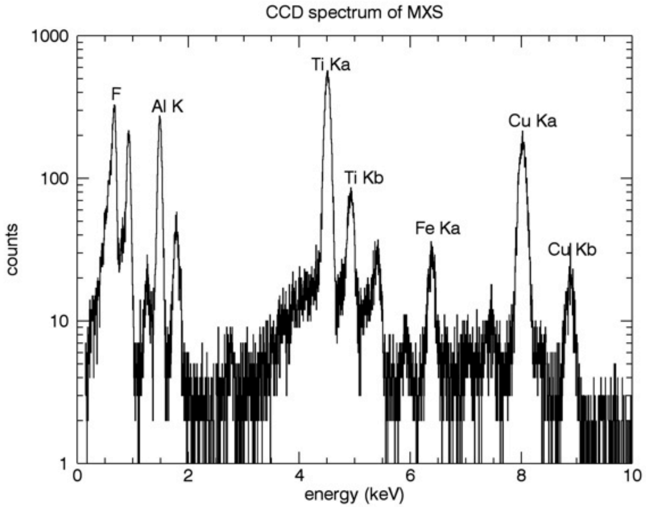

Spectrum of MXS on a CCD

Time delay due to charge drift in SDD

LED pulse producing X-ray flash and voltage step for one of the excited photons

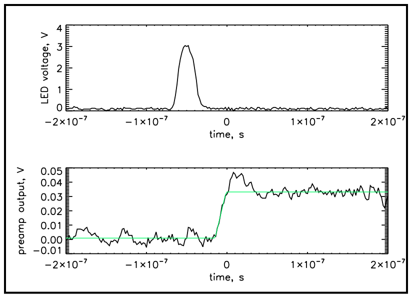

Histogram of step amplitudes for events in the plot above. Ti lines at 4.51 and 4.93 keV are clearly seen

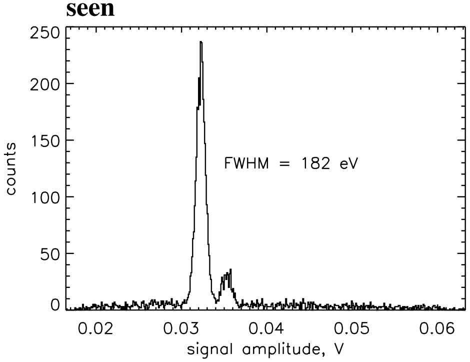

Analyzing large number of events shown on the left, we were able to measure delay time vs position

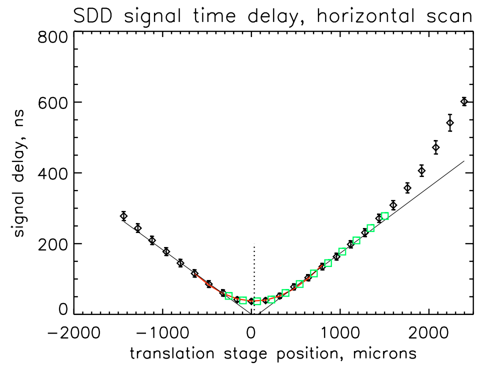

Another byproduct of the same analysis was rise time vs position on the detector

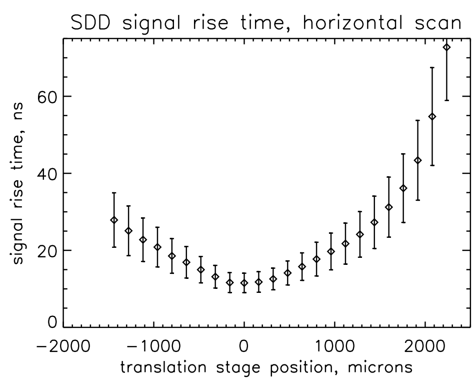

Combining the two results on the left produced a measurement of rise time as a function of delay time. This dependence is a basis for discriminating events originating far from detector center

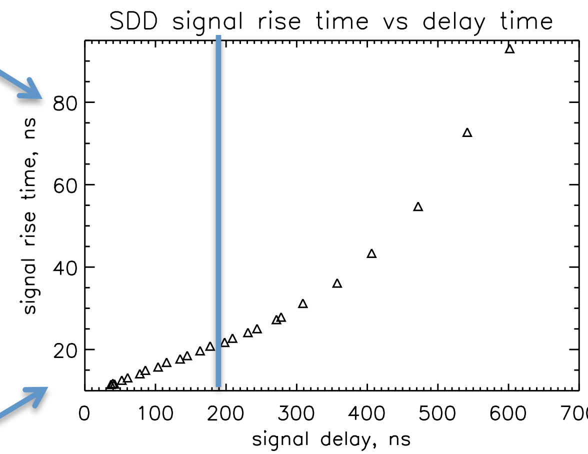

Radiation Testing

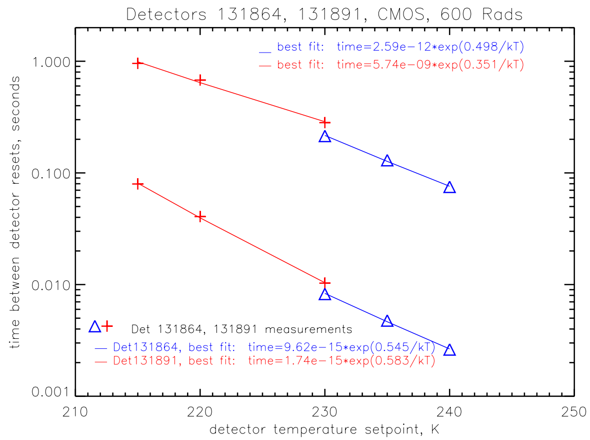

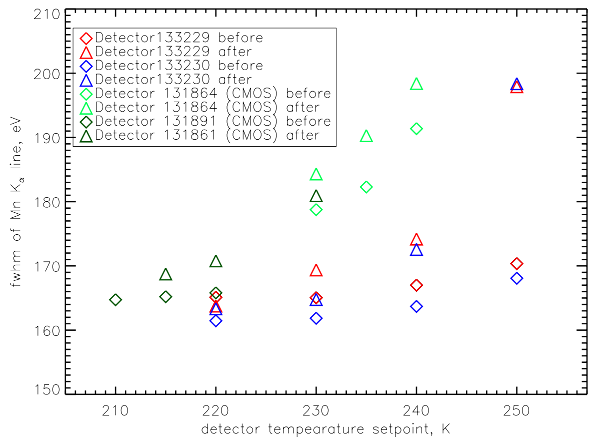

- Both standard SDD and SDD with CMOS preamp were irradiated at the MGH cyclotron to the same dose, 600 Rads of 38 MeV protons. Proton fluence was 3×10^9 protons/cm^2.
- At this dose, which is estimated to be 10 times the dose after 2 years of flight, all devices showed about the same dark current increase of about a factor of 20.
- For all the devices FWHM of the Mn X-ray line was measured before and after irradiation. Results for 600 Rad dose are shown on the left.
- Increase in energy resolution at warmer temperatures after irradiation is caused by extra dark current-associated noise. Estimates of FWHM degradation are in very good agreement with calculations of extra noise due to dark current accumulation during the peaking time of the shaper.
- For chosen temperature of operation (-55C = 218K) energy resolution stays the same as it was before 600 Rad irradiation.

backup

Launch in August 2014

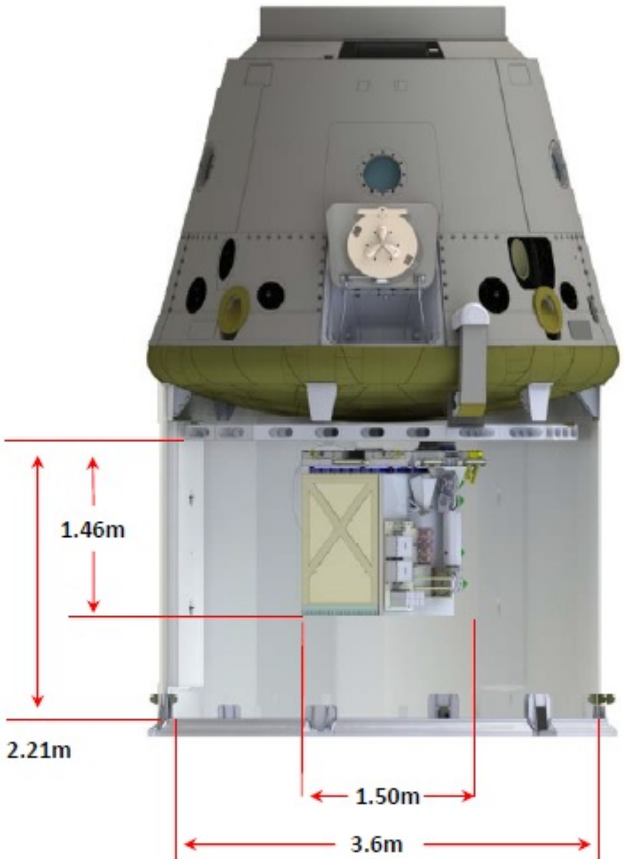

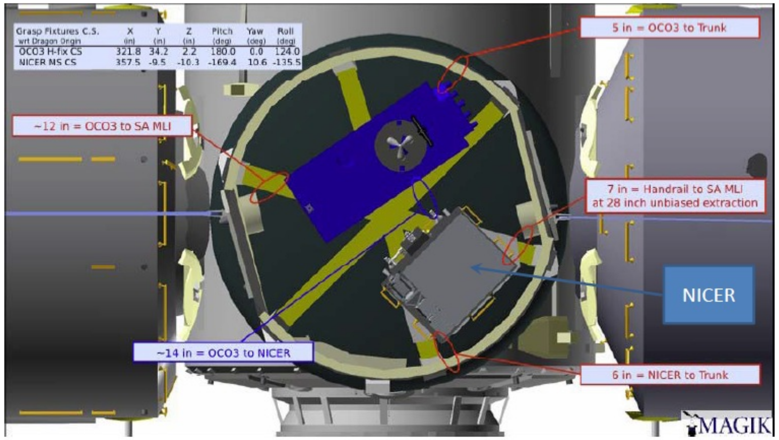

Orthographic View Looking ISS Zenith

- NICER is manifested with one other payload, OCO3, on SpaceX-12 *Falcon 9* launch
- NICER is an unpressurized payload located in the open-ended "trunk" cargo bay
- *Dragon* transport vehicle provides 120 V heater power during transport but no telemetry or 28 V power for electronics
- While docked on the ISS, *Dragon* can provide additional heater power for pre-heating after OCO3 is removed.

- No EVA activities needed to install, deploy, or stow NICER
  - NICER supports 6-hour unpowered survival
- [A] EOTP's PFRAM interface provides pre-heat power and telemetry while berthed
  - [B] NICER is translated to ELC2 Site 7 (outboard ram).

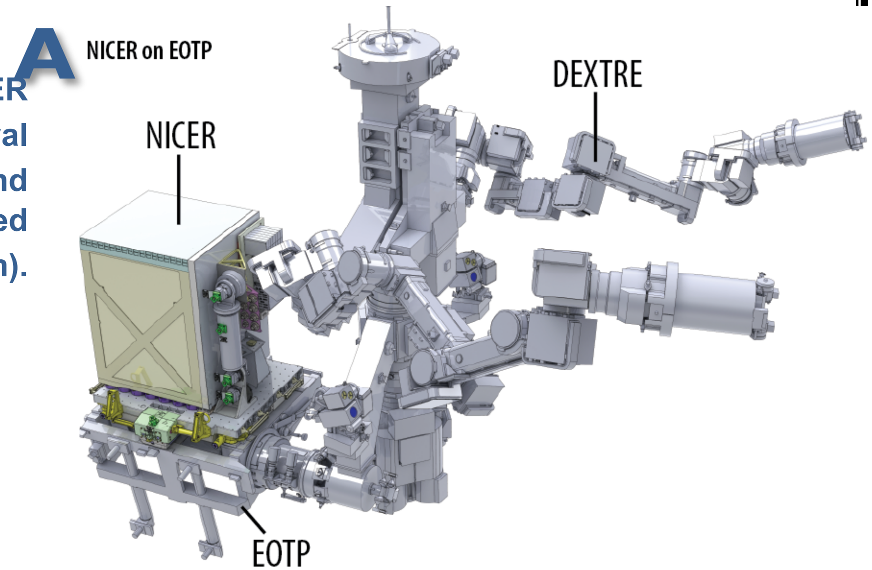

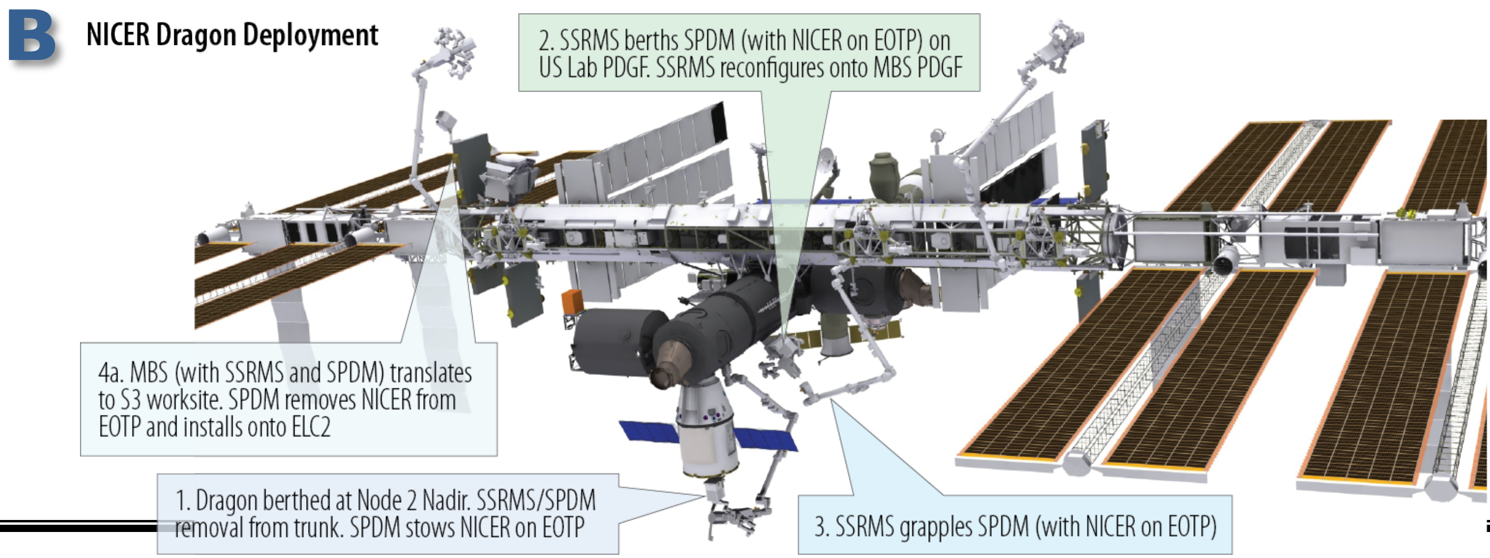

current schedule dates

- CDR 9/16/14
- deliver FMPs 3/27/15
- deliver MPUs 5/11/15
- XTI integration and test finish 7/13/15
- launch 8/11/16

SDD with low energy source (teflon illuminated by Americium with fe55)

energy (keV)	center (adu)	err	fwhm (eV)
5.89	10806.05	0.05	143.47
6.49	11924.79	0.13	150.15
4.75	8674.46	1.87	166.63
4.15	7489.50	0.74	129.97
1.74	2908.27	1.36	95.32
0.68	902.44	0.03	82.17
0.52	640.30	0.16	254.88
0.28	172.07	0.05	94.17